Lattice Model Simulation of Penetrant Diffusion along Hexagonally Packed Rods in a Barrier Matrix As Determined by Pulse-Field-Gradient Nuclear Magnetic Resonance

Guoxing Lin,* Darryl Aucoin, Marcus Giotto, Alana Canfield, Wen-Yang Wen, and Alan A. Jones†

Carlson School of Chemistry and Biochemistry, Clark University, Worcester, Massachusetts 01610

Received November 14, 2006; Revised Manuscript Received January 4, 2007

ABSTRACT: The structural influence on translational diffusion of 2,2,4-trimethylpentane (TMP) through SEBS triblock polymer (poly(styrene)-*block*-poly(ethene-*co*-but-1-ene)-*block*-poly(styrene)) was studied using pulse field gradient (PFG) NMR coupled with lattice model simulation. Two types of PFG experiments were performed: one observing the time-dependent apparent diffusion constant and another observing the diffusion-induced NMR signal attenuation. TMP is selectively sorbed into the rubbery ethylene/butylenes (EB) phase while the glassy poly(styrene) (PS) phase acts as a barrier to TMP diffusion. The observed apparent diffusion constant drops drastically at the grain boundary, in which the orientation of the minor EB cylinder phase changes from grain to grain. In the lattice model simulation, in order to match the large drop of diffusion constant, the diameter of the EB cylinder at the interface had to be reduced by a factor of about 0.7. This extra restriction in the size of the conductive phase indicates the important role of the grain boundary on diffusion in membrane applications of block copolymers. The simulation also shows that the grain boundary influence on diffusion becomes significant when the solubility and diffusivity of the penetrant are greatly different between the rubber and glass phases. In addition, we extended the lattice model to simulate the diffusion-induced PFG NMR signal attenuation. From the simulation and theoretical fitting, it is obvious that the EB phase at grain boundary is not connected well, which is in agreement with our observation of a drastic apparent diffusion constant drop at the grain boundaries in the PFG experiment.

Introduction

The influence of polymer structure on the penetrant translational motion may be studied by observing the time dependence of the diffusion coefficient. The dependence of the apparent diffusion constant on the diffusion time can be directly monitored by pulse field gradient (PFG) nuclear magnetic resonance (NMR).[1] The effects of structural heterogeneity on diffusion have been reported in random copolymers,[2−4] polymer blends,[5] nanocomposites,[6,7] and dispersed oil drops in polymers.[8] In those systems, the structure is not regular or well-defined, so it would be informative to observe penetrant diffusion in a strongly segregated block copolymer with a well-defined morphology. The effect of morphology on diffusion in block copolymers has been examined before by means of sorption,[9] but NMR can directly monitor the dependence of diffusion over a range of length scales. PFG NMR has been used to investigate the diffusion of block copolymers in solution;[10,11] in contrast, the polymer system studied here is in the solid phase.

In this study, the self-diffusion of 2,2,4-trimethylpentane (TMP) in a strongly segregated triblock copolymer poly(styrene)-*block*-poly(ethene-*co*-but-1-ene)-*block*-poly(styrene) (SEBS) was measured by PFG NMR. The SEBS polymer studied had 65 wt % styrene in the end block; thus, the expected morphology consists of hexagonally packed rubbery ethylene/butylene (EB) rods in a glassy polystyrene (PS) matrix.[12−14] This type of triblock copolymer is a potential alternative to Nafion as a permselective membrane for chemical protection and fuel cell applications. It has been shown that partially sulfonated poly(styrene-*block*-(hydrogenated butadiene-*co*-styrene)-*block*-styrene) can serve as a selective membrane that allows for rapid water permeation and slower permeation of chemical warfare simulants.[15] In addition, it has been reported that this type of membrane shows selectivity for proton/water transport vs methanol, appropriate for fuel cell applications.[16] The TMP has a low solubility in PS, measured as 2.85 wt %, and a high solubility in EB rubber, ∼625 wt %; its solubility is 227 wt % in the SEBS triblock. The diffusion of TMP is expected to be of the order of 10^{-7} cm^2 s^{-1} in the EB rubber[17] and 10^{-14} cm^2 s^{-1} in the glassy PS.[18] The combination of those differences in the solubility and diffusion rates assures that the conductive phase will be the EB rubber and the surrounding PS will act as a barrier, which makes TMP in SEBS an ideal system for observing the influence of morphological structure on penetrant diffusion.

Effective medium theory (EMT) has been applied to predict the effective diffusion constant of penetrants in block copolymer systems with different morphologies such as spheres, cylinders, and lamellae.[19] However, EMT cannot predict the dependence of the apparent diffusion constant on the diffusion time. In addition, EMT neglects the effect of the phase continuity across the grain boundary. In the reported CO_2 gas permeability investigation, the EMT prediction agrees well with the experimental results, and in this case, the neglect is justified since the difference in CO_2 gas solubility and diffusion rate is not large enough between the two components of the reported SB copolymer.[9] However, the influence of phase connectivity on TMP diffusion in SEBS may be significant. In the reported PFG results, the apparent diffusion constant of TMP in SEBS has a drastic drop at the grain boundary, which is beyond that predicted by EMT.[20] As mentioned above, the difference in

* To whom correspondence should be addressed. E-mail: glin@clarku.edu.

† Posthumous.

10.1021/ma062619c CCC: $37.00
Published on Web 02/10/2007

solubility and diffusion rates of TMP in rubbery EB phase and in glassy PS phase is large, which will make the influence of grain boundary morphology on diffusion significant if the EB in one domain is not well connected to the EB in the next domain at the grain boundary.

There are reports describing the diffusion in tortuous systems produced by the presence of impenetrable regions.[21−23] However, in the copolymer system, both phases may be penetrable, and each copolymer grain may be penetrable even if one copolymer phase is impenetrable. For a case such as this, we are not aware of other models that could predict the apparent diffusion coefficient at different times, which, fortunately, can be observed via PFG NMR.

In the PFG NMR experiment, the diffusion-induced NMR signal attenuation is closely related to the morphological structure of the studied system. Some analytical expressions have been obtained to relate the diffusion to the NMR signal attenuation and experimental parameters in different systems. They include free diffusion and diffusion inside some regular structures such as single sphere, cylinder, and planar structure.[24−26] However, it is difficult to obtain the analytical expression for complex geometric structures.

A lattice model has been developed to simulate diffusion in heterogeneous polymer membrane systems.[27] This simulation model is based on a model presented by Ediger et al.,[28] which was developed to clarify the physical basis for the apparent enhancement of translational diffusion relative to the rotational motion in glass. In the application to date, a two-domain morphology is constructed on a cubic lattice. One of the domains is associated with fast diffusion and the second domain is associated with slow diffusion. This model has been applied to diffusion in dynamically heterogeneous polymer blends and to a high permeability fluorinated copolymer. In those systems, the initial morphology is a random distribution of fast and slow domains. For the block copolymer systems, the morphology will consist of a well-established structure of spheres, lamella, and cylinders.[12] To improve our understanding of penetrant diffusion in block copolymers and better interpret the PFG NMR diffusion experiment, the lattice model[27] is modified to simulate the time-dependent diffusion process. The routine of building the lattice with randomly oriented and randomly sized grains is outlined, and the grain boundary influence on diffusion is simulated. In addition, we also extend the lattice model to simulate the diffusion-induced PFG NMR signal attenuation, which was performed by directly recording the nuclear spin phase change resulting from magnetic field gradients during the penetrant random walk. The simulated signal attenuation is compared with theoretical results from short-gradient-pulse (SGP) approximation for diffusion in the cylindrical structure.

Experiment and Results

SEBS triblock polymer, poly(styrene)-*block*-poly(ethene-co-but-1-ene)-*block*-poly(styrene) with a molecular weight of 49K and styrene end blocks of 16K, was provided by Drs. Donald Rivin and Nathan S. Schneider of the Natick Soldier Center. The SEBS film was prepared by casting from a 5 wt % solution of the triblock in toluene. The solution was evaporated from a Mylar sheet, leaving a film with a thickness of about 100 μm. The film was then cut into small pieces, placed into an 8 mm NMR tube with 20 wt % TMP, and sealed under vacuum. PFG measurements were performed on a Varian Inova 400 MHz wide-bore NMR spectrometer in an 8 mm direct detection probe with high gradient capability (1000 G/cm) from Doty Scientific. Glass spacers were placed in the NMR tube to center the sample in the region of the radio frequency and gradient coils.

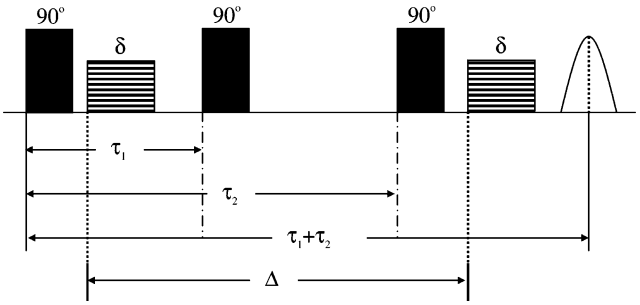

Figure 1. Pulse sequence used for the measurement of proton translational diffusion. The gradient pulse width δ is typically 1 ms, and the time Δ over which diffusion occurs can be varied from 3 to 1000 ms.

Using proton NMR, the apparent diffusion constant of the penetrant, D_{app}, was measured at 26 °C as a function of the time over which self-diffusion occurs in the stimulated echo pulse sequence, Δ, as shown in Figure 1. The apparent diffusion constant in the PFG NMR experiment is defined by[29]

$$D_{app}(\Delta) = -\frac{1}{\gamma^2\delta^2(\Delta - \delta/3)} \lim_{g\to 0} \frac{\partial \ln E(g^2,\Delta)}{\partial g^2} \qquad (1)$$

where $E(g^2,\Delta)$ is the echo amplitude, γ is the gyromagnetic ratio, g is the gradient strength, and δ is the duration of gradient pulse. Only the initial decay of echo amplitude was monitored, typically to a level of about 70% of the original amplitude. At a given time Δ, the gradient amplitude, g, was varied from 0 to up to a few hundred G/cm. The time Δ, ranged from 4 ms to 1 s. The length of the gradient pulses was fixed at 1 ms. The apparent diffusion constant at a given value of Δ is calculated from the slope of a plot of the logarithm of the echo amplitude vs g^2. The results of 10, 20, and 24 wt % TMP diffusion are shown in Figure 2.

In Figure 2, the apparent diffusion constant D_{app} for the TMP in the SEBS is plotted as a function of the average root-mean-square displacement ($\langle r^2\rangle^{1/2}$), which is given by the equation $\langle r^2\rangle^{1/2} = \sqrt{6D_{app}\Delta}$. This value represents the average distance that a TMP molecule diffuses in a time Δ, assuming an isotropic medium. In the PFG experiment, diffusion is observed in the direction of the magnetic field gradient, and the medium is a sum over all orientations of the EB domains relative to the field. At short time, the medium is anisotropic but at longer time diffusion will average over the structure. This anisotropy is due to copolymer morphology, which is different from that induced by deformation of polymer networks with increasing compression force.[30] This average is roughly achieved since D_{app} approaches a plateau at large values of $\langle r^2\rangle^{1/2}$. This same general behavior is observed in SEBS samples at a variety of concentrations of TMP in the 10−24 wt % range.

The TMP diffusion is fast at short time and slows down as time increases. The fast diffusion constants occurring inside the EB phase are in the range of 10^{-7} cm^2 s^{-1}, as would be expected for a rubbery matrix. When the TMP makes contact with the PS at the walls of the EB domain, D_{app} decreases. The EB phase swollen by the penetrant has a diameter in the range of tens of nanometers but a length in the range of microns.[31] The latter is determined by the grain size, a second morphological characteristic affecting diffusion. Together these two distances determine the length scale for the initial contact with the PS. The initial contacts occurring on the length scale of the diameter is too short to be observed by PFG NMR with gradients in the range of 1000 G/cm. The diffusion drops an order of magnitude between 2 and 5 μm due to the length scale of the grains. Cast

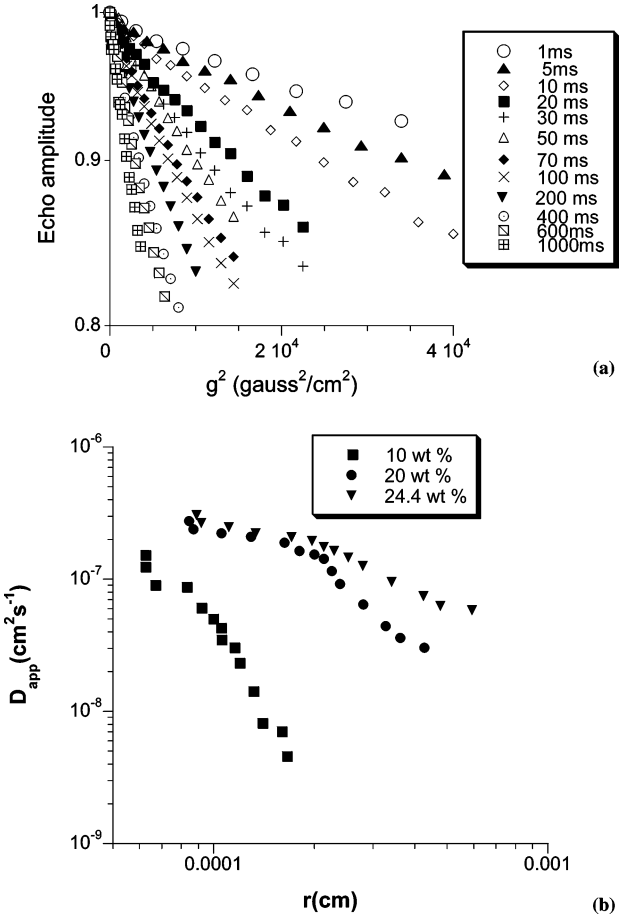

Figure 2. (a) Echo amplitude vs gradient square for 20 wt % TMP in the SEBS triblock copolymer. (b) The apparent diffusion constant as a function of square root of mean-square displacement of TMP molecules in the PFG NMR experiment for three different concentrations of TMP in the SEBS triblock copolymer.

films of block copolymers of this type commonly have grain boundaries[32] between domains where the orientation of the EB phase changes. At the interface, the EB in one grain may not be well connected to the EB in the next grain. Various types of dislocations have been observed and described for the block copolymer morphology at a grain boundary.[32] In general, there could be a narrowing of the connections between cylinders or lamella at the boundary if not an outright disconnection. In any of these cases, diffusion will be impeded leading to a drop in the D_{app}. Since there is a distribution of grain sizes and orientations in any real sample, the drop is spread out over a range of sizes, which is about 2 to 5 μm in our experiment.

In a separate experiment, the diffusion-induced NMR signal attenuation was measured at 26 °C with diffusion time Δ equaling 200 ms and a gradient pulse width of 3 ms. Gradient amplitude, g, was varied from 0 to up to 900 G/cm. The result is shown in Figure 3.

Variable temperature ^{2}H spin−lattice relaxation measurements of TMP were performed on two Varian NMR spectrometers: a Varian Inova wide bore 400 NMR spectrometer (61.4 MHz) and a Varian Mercury narrow bore 200 NMR spectrometer (30.7 MHz). These are shown in Figure 4.

Diffusion Simulation

The basic procedure of lattice molel simulation has been described in detail by the Ediger group and Jones group,[27,28] which will not be repeated here. We will pay more attention to the building of the random lattice and simulation results.

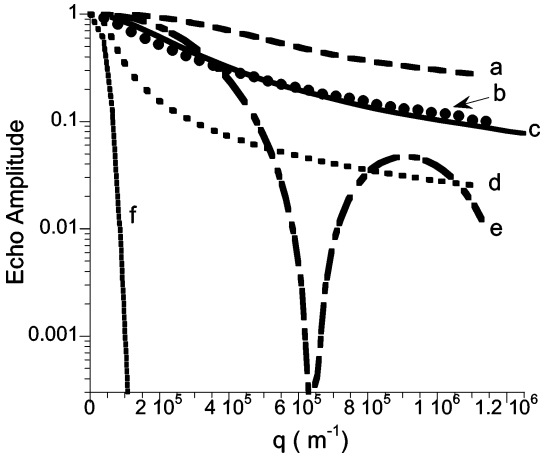

Figure 3. Echo amplitude vs q: (a) spatial averaging over randomly oriented cylinders with $R \rightarrow 0$ and $L = 1.6$ μm; (b) PFG experiment; (c) lattice model simulation; (d) Fickian-like diffusion, spatial averaging over randomly oriented cylinder with $R \rightarrow 0$ and $L \rightarrow$ infinite; (e) cylinder with symmetric axis angle $\theta = 0$, $R \rightarrow 0$, and $L = 1.6$ μm; (f) Fickian diffusion in homogeneous medium.

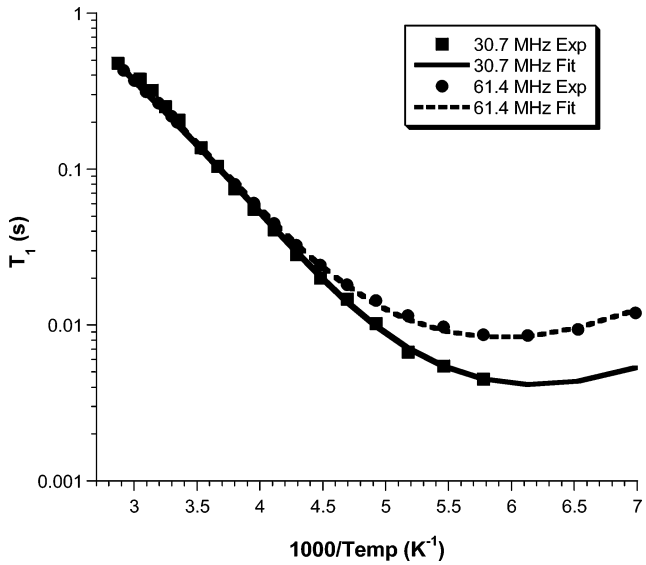

Figure 4. Deuterium T_1 for deuterated TMP in SEBS. Curves are fitted in terms of rotation correlation times with a single modified KWW distribution.

(1) 3D Random Hexagonally Packed Cylinder Lattice. Figure 5 shows the cartoon of the lattice model used for the simulation of TMP diffusion in SEBS triblock copolymer. The three-dimensional lattice in the simulation consists of $(1024)^3$ small cubic boxes. Each EB cylinder has a diameter of 8 cubic boxes. For SEBS, the rubber EB phase and glass PS phase are specified by two different types of small cubic boxes: one with fast diffusion constant (1.29×10^{-6} cm^2 s^{-1}) representing the dispersed EB cylinder phase and another with very slow diffusion (1.29×10^{-9} cm^2 s^{-1}) representing the continuous PS phase. The diffusion inside each polymer phase is assumed homogeneous. To maintain the difference of TMP solubility between EB and PS phase, microreversibility at their interface is set to produce the concentration gradient.[27] Periodic boundary conditions are used in the lattice.

The lattice with randomly oriented and randomly sized, hexagonally packed cylinder grains is built step by step. First, the cubic lattice is divided into random sized grains. In the 3D

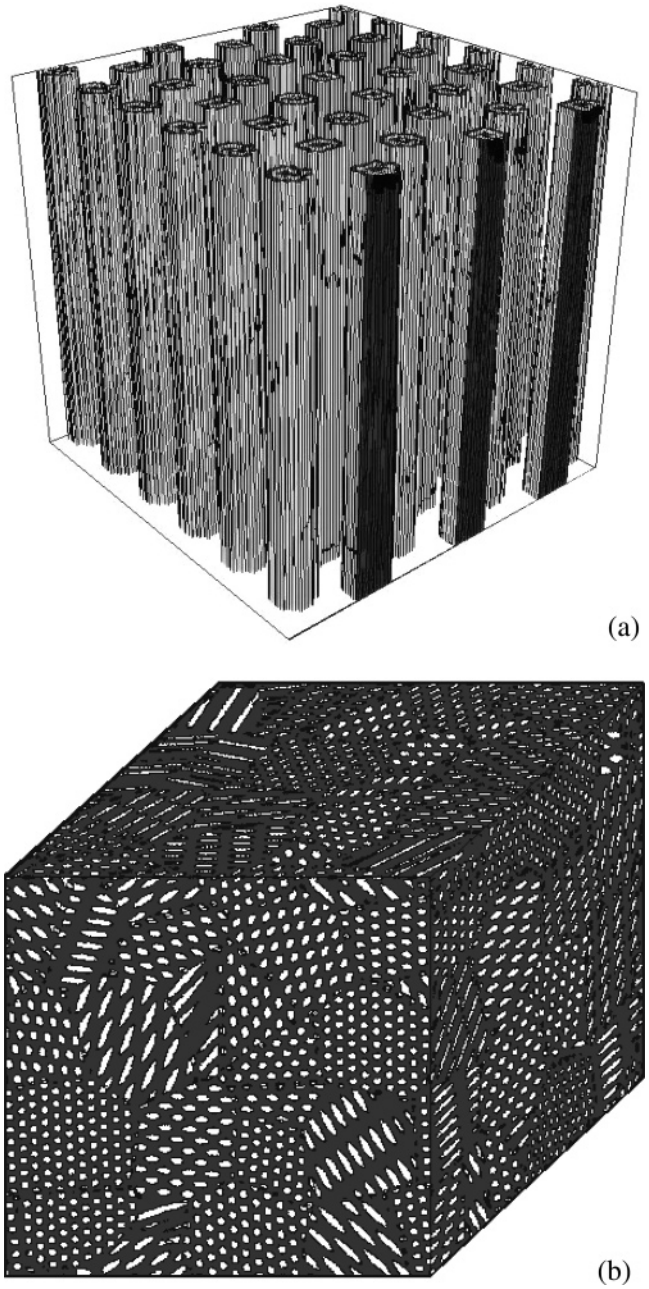

Figure 5. Three-dimensional hexagonally packed cylinders lattice structures: (a) regular structure; (b) randomly oriented and randomly sized polygonal grain structure.

cubic lattice, we randomly pick some points as grain centers. The total number of grain centers $N_{\text{grain centers}}$ is calculated by

$$N_{\text{grain centers}} = \frac{V_{\text{total}}}{\bar{v}_{\text{grain}}} \tag{2}$$

where V_{total} is the total volume of the lattice and $\bar{v}_{\text{grain}}$ is the average grain volume. Each cubic box belongs to a grain whose grain center is nearest to the cubic box in the lattice. By this way, the grain will be a random polygon with random size.

Second, for each grain we perform one Euler rotation around its grain center with a random Euler angle (α,β,γ). Each cubic box in the rotated grain will correspond to a cubic box in an unrotated regular cylinder lattice that we built for reference. The rotated cubic box is assigned the same phase as that of the referenced cubic box, which was given when the referenced lattice was built and will not be changed. Hence, the orientation of each grain will be random, depending on the random Euler angle.

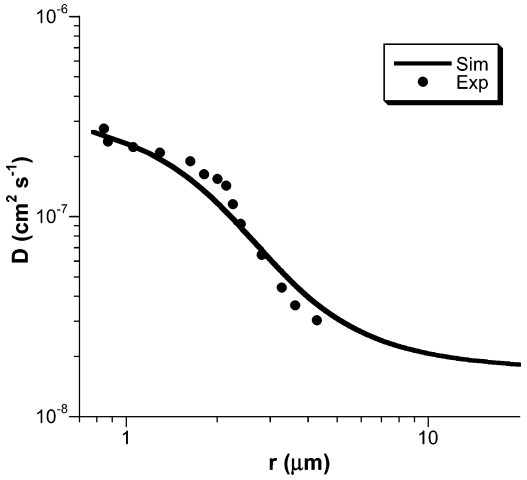

Figure 6. Comparison of apparent diffusion constant as a function of root-mean-square displacement from lattice model simulation of diffusion and the experimental results. Grain size from the simulation is 2.5 μm.

Other geometric structures can be built by this same method, allowing for simulation of diffusion in the sphere and lamella systems.

(2) Simulation of Time-Dependent Apparent Diffusion. To simulate diffusion, random walks were performed on the lattice built previously. In each random walk, at time t, the spatial position $r(t)$ was recorded. The simulated apparent diffusion constant was calculated by $D_{\text{app}} = \langle r^2 \rangle / 6t$. In the simulation, the two adjustable parameters, TMP diffusion constant in EB phase and the grain size, were used. The actual value of the diffusion constant in the PS domains is not important in the simulation as long as it is more than about 3 orders of magnitude smaller than the diffusion constant in the EB domain, so the TMP diffusion constant in PS phase is set as 1000th of that in EB phase. The solubility difference from permeability measurement is used in the simulation. In the simulation, the diffusion constant in EB phase was mainly determined by the short time diffusion constant obtained from the PFG experiment. It is determined to be 1.29×10^{-6} cm^2 s^{-1}, very close to the TMP diffusion constant in the 87% EB and 13% PS triblock copolymer that we measured. The experimental and simulated short time apparent diffusion coefficients of TMP are about one-third of that in the pure EB phase. The simulation results compared with experimental results are shown in Figure 6, which is the average of over 3000 random walks. To get the order of magnitude decrease in the apparent diffusion constant, the diameter of the cylinder at the interface had to be reduced by a factor of about 0.7. When the effect of all orientations is considered, effective medium theory predicts a factor of $^1/_3$ reduction in the diffusion constant of TMP in SEBS. To match the experimental results, the extra restriction in the size of the conductive phase at the grain boundary must be added. This indicates an important structural characteristic of the interface between grains. The grain size determined by the simulation is 2.5 μm, which is mainly determined by the position where the experimental diffusion constant drops drastically (Figure 6). The same simulation parameters match another view of the experimental results, as shown in Figure 7. Here, the mean-square displacement is plotted vs the time over which diffusion is observed in the pulse field gradient diffusion experiment. The mean-square displacement grows rapidly at short times and then

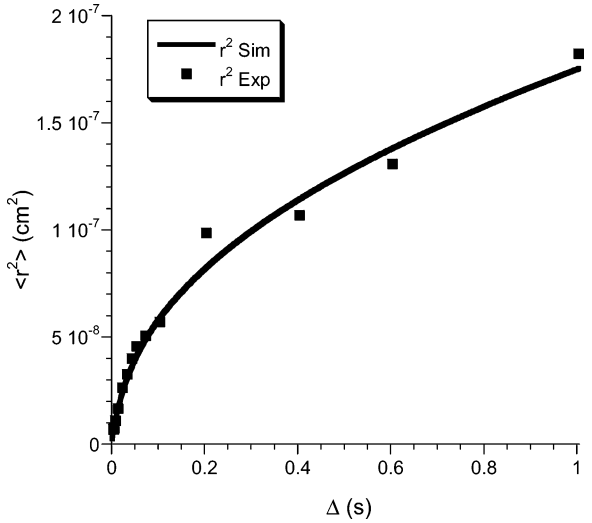

Figure 7. Mean-square displacement vs the time over which diffusion is observed in the PFG NMR experiment. Experimental results are compared with the simulation.

slows at longer times. This reflects rapid diffusion inside an EB cylinder which slows as the TMP molecules encounter the PS phase where diffusion is slower and solubility is lower.

Earlier investigations based on CO_2 gas permeability showed that grain boundary does not greatly affect the diffusion; however, the influence of the grain boundary on TMP diffusion in SEBS is significant. The two diffusion processes are quite different. In the SEBS system, the TMP solubility in EB rubber phase is more than 200 times higher than that in polystyrene and the TMP diffusion constant in EB rubber is more than 1000 times higher than that in the PS phase. In the reported result, the CO_2 gas solubility in the rubber phase is about 40% of that in PS, and the diffusion constant in rubber phase is about 63 times higher than that in the PS phase. When the penetrant diffusion is impeded by the dislocation of fast diffusion phase at grain boundary, the penetrant can continue its diffusion by entering another phase if the solubility and diffusion constants between those two phases are not very different; otherwise, the penetrant diffusion will greatly slow down. The role of solubility ratio and difference in diffusion constants in the influence of grain boundary on the diffusion can be simulated by the lattice model. The simulation results are shown in Figure 8. From the results, we can see that the smaller the solubility difference, the smaller is the influence of grain morphology. In addition, we can see that when the solubility and diffusion constant differences are small, the penetrant diffusion has already averaged over the structure at very short length before the penetrant diffuses to the grain boundary; thus, we do not see significant grain boundary influence on the diffusion. This is in agreement with the reported situation in the CO_2 gas permeability. When the diffusion and solubility difference increases, the grain boundary influence becomes more and more significant. This is in agreement with our PFG experiment.

(3) Simulation of PFG-Induced NMR Signal Attenuation. From the simulation in the above section, it has been shown that the EB cylinder phase at the grain boundary is not well connected. In the following, we try to investigate the structure influence on the diffusion from a different way by studying the PFG-induced NMR signal attenuation.

In PFG NMR experiment, the magnetic field gradient pulse creates a spatial phase distribution structure of nuclear spins. The displacement of nuclear spins resulting from the translational diffusion will cause the mixing of spins with different phases and lead to NMR signal attenuation. The signal amplitude attenuation gives information on the displacement along the gradient axis. The displacement of penetant is affected by the morphology of the system studied. Particularly, with large q value ($q = \gamma g\delta/2\pi$), diffusive diffraction can be observed for spins trapped in a closed pore at long diffusion time limit in PFG experiment.[1,29] To see the morphology influence on the NMR signal and to see whether we can observe the diffusive diffraction effect at long time limit, the stimulated echo PFG experiment was performed with Δ equaling 200 ms, which satisfies the condition $D\Delta \gg L^2$ (D is the short time diffusion constant and L is the size of geometric structure). The experimental results are shown in Figure 3, which can be analyzed by different situations as described in the following.

In the SEBS triblock copolymer, if the EB cylinder phases at different grains are connected very poorly at the grain boundary, the diffusion may be treated as restricted diffusion. When the symmetry axis of a cylinder takes an arbitrary angle with respect to the direction of magnetic field gradient, the PFG NMR signal attenuation $E(q,\Delta)$ in a closed cylinder is given by[26]

$$E(q,\Delta,\theta) = \sum_{n=0}^{\infty}\sum_{k=1}^{\infty}\sum_{m=0}^{\infty} \frac{2K_{nm}R^2(2\pi qR)^4\sin^2(2\theta)[1-(-1)^n\cos(2\pi qL\cos\theta)]\alpha_{km}{}^2}{L^2[(n\pi R/L)^2-(2\pi qR)^2\cos^2\theta]^2[\alpha_{km}{}^2-(2\pi qR)^2\sin^2\theta]^2(\alpha_{km}{}^2-m^2)} [J'_m(2\pi qR\sin\theta)]^2\exp\left\{-\left[\left(\frac{\alpha_{km}}{R}\right)^2+\left(\frac{n\pi}{L}\right)^2\right]D\Delta\right\}$$

$$K_{nm}=1 \quad \text{if } n=m=0$$

$$K_{nm}=2 \quad \text{if } n\neq 0 \text{ and } m=0 \text{ or } m\neq 0 \text{ and } n=0$$

$$K_{nm}=4 \quad \text{if } n,m\neq 0 \qquad (3)$$

where L and R are the length and radius of the cylinder, respectively, α_{km} is the root of equation $J'_m(\alpha) = 0$ (J is the Bessel function of the first kind, with the convention that $\alpha_{10} = 0$), and $q = \gamma g\delta/2\pi$, in which γ is the gyromagnetic ratio, g is the gradient strength, and δ is the duration of gradient pulse.

In the SEBS copolymer, the EB cylinder is a long thin nanotube with a diameter of about 20 nm estimated from self-consistent mean-field theory,[31] which indicates $D\Delta \gg R^2$ in our PFG NMR experiment. Thus, by eliminating radially related terms (R, J, α_{10} and m) originating from the Bessel equation, eq 3 can be reduced to

$$E_{R\to 0}(q,\Delta,\theta) = \frac{2[1-\cos(2\pi qL\cos\theta)]}{(2\pi qL\cos\theta)^2} + 4(2\pi qL\cos\theta)^2\sum_{n=1}^{\infty}\exp\left(-\frac{n^2\pi^2D\Delta}{L^2}\right)\frac{1-(-1)^n\cos(2\pi qL\cos\theta)}{[(2\pi qL\cos\theta)^2-(n\pi)^2]^2} \qquad (4)$$

In eq 4, the cylinder radius does not appear. The structure parameters affecting signal amplitude are cylinder length and symmetric axis direction angle θ. When the angle equals 0, this equation reduces to the signal attenuation within planar boundaries. It is reasonable that the planar structure can be considered as an ensemble of enormous parallel thin cylinders. In those cylinders, the one-dimensional diffusion along the direction of

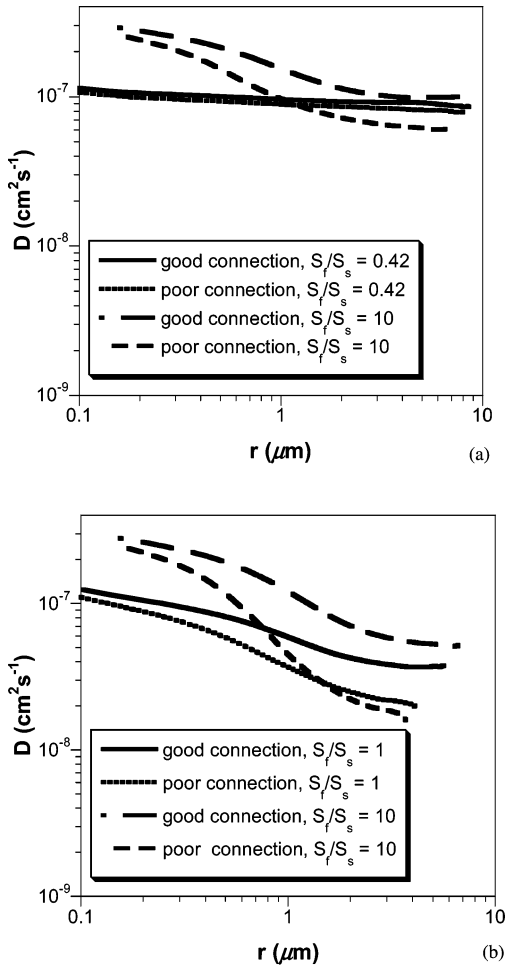

Figure 8. Diffusion constant vs the length scale with different diffusion constant and solubility ratios between the fast and slow phases: (a) D_f:D_s = 63; (b) D_f:D_s = 1000. The grain size used in the simulation is 1 μm.

the symmetric axis is the same as that in the planar structure, so they have the same PFG signal attenuation expression. Another way to consider the signal attenuation expression for the cylinder in an arbitrary direction can be obtained from the expression for planar structure by projecting the penetrant displacement and distance parameter onto the gradient direction, with replacement $D\Delta \rightarrow D\Delta \cos^2\theta$, $L \rightarrow L \cos\theta$. Averaging over all the orientations, the total signal attenuation will be

$$S_{\text{total}}(q,\Delta) = \frac{\int_{\theta=0}^{\pi} E_{R\rightarrow 0}(q,\Delta,\theta) \sin\theta \, d\theta}{\int_{\theta=0}^{\pi} \sin\theta \, d\theta} \tag{5}$$

If the EB cylinder phase between different grains is connected very well, the penetrant will diffuse like Fickian diffusion in the EB phase. Though the penetrant diffusion changes direction when diffusing from one grain to another grain, this only affects the diffusion speed. Such a diffusion process can be treated approximately as one-dimensional Fickian diffusion. The spatial average signal attenuation can be given by[33]

$$S_{\text{total}}(q,\Delta) = \frac{\int_{0}^{\pi} \exp[-(2\pi q)^2 D\Delta \cos^2\theta] \sin\theta \, d\theta}{\int_{0}^{\pi} \sin\theta \, d\theta} \tag{6}$$

Equations 5 and 6 describe two extreme diffusion situations: one with poor connection and another with good connection at the grain boundary. The real connection may be quite different. In the apparent diffusion constant simulation, the diameter of the cylinder at the interface had to be reduced by a factor of about 0.7. The lattice configuration used in above section can be modified to simulate the experimental signal attenuation. In the lattice simulation, the spatial position as a function of time, $z(t)$, has already been recorded during the random walk, so at time t the phase change of spin in the ith walk, $\phi_i(t)$, can be calculated by

$$\phi_i(t) = \sum_{t_j=0}^{t} \gamma g(t_j)\, z(t_j) \delta_t \tag{7}$$

where γ is the gyromagnetic ratio, $g(t_j)$ is the gradient strength, and δ_t is the time increment at time t_j. The signal attenuation resulting from the finite field gradient pulse duration effect[24] can be easily included in eq 7. The total normalized signal attenuation will be

$$E(q,\Delta) = \frac{1}{N} \sum_{i=1}^{N_{\text{walks}}} \cos[\phi_i(\Delta)] \tag{8}$$

The fitting of eqs 5 and 6 and lattice simulation results are compared with experimental results as shown in Figure 3. In the experiment, as we mentioned above, only one diffusion time Δ equaling to 200 ms was used, and in order to get the large q value for diffusive diffraction effect, the gradient pulse width used is 3 ms and the gradient amplitude, g, was varied from 0 to up to 900 G/cm. In the fitting and simulation, the parameters Δ and q from PFG experiment and the diffusion constant D for EB phase determined from simulation of the last section, 1.29 $\times$ 10^{-6} cm^2 s^{-1}, were used. Actually, the NMR signal attenuation at long diffusion time is not sensitive to the short time diffusion constant in restricted diffusion. In a closed pore, the long time limit signal attenuation is only determined by q and pore size. The only adjustable parameter in the simulation in this section is the grain size or the cylinder length. By varying the grain size, it was found that grain size of 1.6 μm makes the simulated signal attenuation very close to the experimental results, which is shown in Figure 3. The grain size 1.6 μm is then used as the cylinder symmetric axis length and substituted into eqs 3−6 to get the cylinder fitting. Though we can use 2.5 μm obtained from the simulation in the last section in the cylinder fitting, it will not affect the analysis result much. The cylinder structure fitting is closer to the experimental results than that of the Fickian diffusion fitting, particularly at the small q, which indicates that the EB phase at the grain boundary is not connected very well in our system. However, the real connection is different from the above; two extremely poor and good connections for the experimental results are away from both fitting curves. The grain size obtained here is 1.6 μm, which is different from 2.5 μm obtained from the apparent diffusion constant simulation in the previous section. The discrepancy stems from that the experimental conditions of PFG apparent diffusion constant measurement and PFG diffusive diffraction measurement are different. In the former, the q value is small, while in the latter, it ranges from small to very large. In the heterogeneous diffusion system, at large q value, the higher order contribution from the displacement will affect the signal attenuation.[1,29] So the two type PFG experiments have different sensitivities in the penetrant displacement. Thus, it is reasonable that two different grain sizes in the simulation were obtained. In general, the PFG echo amplitude vs small q value gives the mean-squared displacement;[29] therefore, 2.5 μm is more accurate

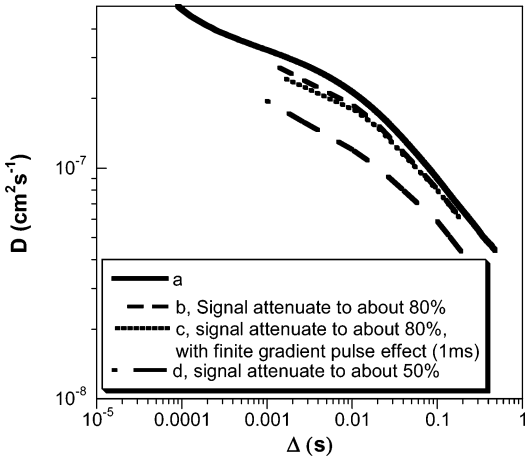

Figure 9. Comparison of the simulated apparent diffusion constant obtained from two different ways. (i) from the mean-square displacement vs time (a); (ii) from the slope of logarithm of echo amplitude vs gradient square (b, c, d).

than 1.6 μm. In Figure 3, the diffraction pattern for cylinders parallel to the magnetic gradient direction is not shown in our experiment because the cylinder here is not a closed system, and the grains have a random size distribution and random orientations.

Additionally, the lattice model simulation can be used to check and choose good experimental conditions for PFG NMR diffusion experiments. In heterogeneous diffusion, when the signal attenuates too much at higher gradient value (q value), the higher order contribution from smaller displacement cannot be neglected and the signal attenuation is not proportional to the mean-square displacement $\langle r^2 \rangle$.[1,29] However, when the signal attenuation is too small, the signal-to-noise will become problematic. Therefore, choosing appropriate signal attenuation is important in the PFG experiment. In the lattice model simulation, the mean-square displacement $\langle r^2 \rangle$ and PFG NMR singal attenuation can be simulated. Therefore, we have two different ways to obtain the apparent diffusion constant in the lattice model simulation. One way is to obtain the apparent diffusion constant from $\langle r^2 \rangle/6t$, from which the apparent diffusion constant is accurately related to the geometric structure size parameter and is assumed the corrected apparent diffusion constant here. Another way is to obtain the appatent diffusion constant by the slope of logarithm of echo amplitude vs gradient square, which is used in the PFG experiment mentioned previously. The apparent diffusion constant obtained in the second way depends on the gradient strength used in the simulation or experiment. The different range of gradient value used in the lattice model simulation has different signal amplitude attenuation. The simulated apparent diffusion constant obtained from the two different ways is shown in Figure 9. The diffusion constant obtained from about 20% signal attenuation agrees reasonably well with the simulated apparent diffusion constant obtained from $\langle r^2 \rangle/6t$. When the signal attenuation increases to about 50%, the diffusion constants become unreliable for it cannot get reasonable size of the geometric structure.

Conclusions

In the system studied the diffusion is tortuous in nature with fast diffusion observed at short times or equivalently small distances. The diffusion is fast in EB phase and very slow in PS phase. The diffusion constants at short length scales are in the range of 10^{-7} cm^2 s^{-1}, as would be expected for a rubbery matrix. Rotational motion characterized by a correlation time τ can be related to the diffusion coefficient D by the equation $D = 2r^2/9\tau$, where r is the molecular size.[28] In Figure 4, a single modified Kohlrausch−Williams−Watts (KWW) correlation function with a Vogel−Fulcher−Tammann−Hesse (VFTH) temperature dependence of relaxation time[34,35] was used in fitting the T_1 experimental results. This indicates that rotational motion of TMP is observed only in the EB rubber domain. The solubility of TMP in the PS domain is too low to be detected in the T_1 experiment. This is consistent with the EB rubber phase serving as the conducting phase as shown in the diffusion measurements.

TMP diffusion is affected by two morphology characteristics, including the cylinder diameter and the grain boundary. The former is too short to be detected by current PFG techniques. The latter is determined by grain size in the range of microns. From the PFG experiment and the lattice simulation, the grain size varies from to 2 to 5 μm, in which the apparent diffusion constant has an order of magnitude decrease. The big drop is beyond that predicted by the effective medium theory. From the lattice simulation, to attain such a big diffusion drop, the diameter of the cylinder at the interface must be reduced by a factor of about 0.7, which indicates that EB cylinder phase in one grain is not well connected to the EB in another grain. This finding is in agreement with the reported dislocations between the cylinders at grain boundary.[32]

The short time D_{app} is about one-third of the TMP diffusion coefficient in the pure EB phase, which supports that the expected SEBS morphology is cylinder structure for the spatially averaged one-dimensional diffusion constant is one-third of the three-dimensional diffusion constant in pure EB phase. If the morphology is lamella, the short time D_{app} of TMP will be about two-thirds of that in pure EB phase and the drop in diffusion constant at the grain boundary will not be big, which is quite different from the observed PFG diffusion results.

The influence of grain boundary on diffusion is closely related to the difference in solubility and diffusion constant between the two components of the block copolymer. When the solubility difference and difference in diffusion constant are small, the penetrant can diffuse in both phases, so the penetrant diffusion will average over the copolymer structure at short length scale and the connection of the rubbery phase at grain boundary has no significant influence on the diffusion. The situation is similar to the reported gas permeability investigation, which can be described by EMT. With the increase in difference of the solubility and diffusion constant difference, the grain boundary influence becomes more and more significant; the penetrant cannot find an alternative path to diffuse if the conductive rubbery phase is not well connected, which leads to a big decrease in the diffusion constant as observed in the PFG TMP diffusion. EMT cannot describe this drop because it neglects the grain boundary connection.

From the comparison of the cylinder structure fitting, the Fickian diffusion fitting, and the experiment signal attenuation shown in Figure 3, it is obvious that signal attenuation from the restricted diffusion in cylinders is closer to the reality than that from Fickian diffusion. This indicates that the TMP molecules in EB cylinder cannot easily diffuse from one grain to another grain. It also indicates that the EB phase at grain boundary is not connected very well in our system. In Figure 3, the experimental result does not show the characteristic diffraction pattern for restricted diffusion in cylinders parallel to the magnetic gradient. This results from that there is random distribution of the grain size and orientation in this system and the system is not a closed system.

Given the observed order of magnitude drop in D_{app}, grain boundaries and grain boundary morphology play an important role in potential applications of block copolymers as membranes. The morphology controlled by relative block size in the triblock copolymer only partially determines transport in an actual membrane. PFG NMR can directly assess the effects of grain boundaries. The lattice model simulation provides a quantitative interpretation of the PFG NMR experiment and improves our understanding of the diffusion process. In addition, our extension of the lattice model to simulate the diffusion-induced PFG NMR signal attenuation leads to a new way to interpret the PFG NMR experiment.

Acknowledgment. This paper is dedicated in memory of Professor Alan A. Jones. This work was supported by the Army Research Office, Grant DAAD19-03-1-0087. The authors thank Drs. Donald Rivin and Nathan S. Schneider for solubility measurements of TMP in PS and the triblock copolymer.

References and Notes

(1) Callaghan, P. T. *Principles of Nuclear Magnetic Resonance Microscopy*; Oxford University Press: New York, 1991.
(2) Meresi, G.; Wang, Y.; Cardoza, J.; Wen, W.-Y.; Jones, A. A.; Inglefield, P. T. Topology of High Free Volume Regions from Pulsed Field Gradient Diffusion Studies of Penetrant Motion in Perfluorodioxole Copolymer. *Macromolecules* **2001**, *34*, 1131−1133.
(3) Meresi, G.; Wang, Y.; Cardoza, J.; Wen, W.-Y.; Jones, A. A.; Gosselin, J.; Azar, D.; Inglefield, P. T. Pulse Field Gradient NMR Study of Diffusion of Pentane in Amorphous Glassy Perfluorodioxole. *Macromolecules* **2001**, *34*, 4852−4856.
(4) Hayamizu, K.; Akiba, E.; Bando, T.; Aihara, Y.; Price, W. S. NMR Studies of Poly(ethylene oxide)-based Polymer Electrolytes with Different Cross-Linkink Doped with $LiN(SO_2CF_3)_2$. Restricted Diffusion of the Polymer and Lithium Ion and Time Dependent Diffusion of the Anion. *Macromolecules* **2003**, *36*, 2785−2792.
(5) Cao, H.; Lin, G.; Jones, A. A. Penetrant Diffusion as a Probe of Local Compositional Structure in a Blend of Poly(ethylene oxide) and Poly(methyl methacrylate). *J. Polym. Sci., Polym. Phys.* **2004**, *42*, 1053−1067.
(6) Zhong, J.; Wen, W.-Y.; Jones, A. A. Enhancement of Diffusion in a High Permeability Polymer by the Addition of Nanoparticles. *Macromolecules* **2003**, *36*, 6430−6432.
(7) Zhong, J.; Lin, G.; Wen, W.-Y.; Jones, A. A.; Kelman, S.; Freeman, B. D. Translational and Rotational Motion of Penetrants in Ultrapermeable Nanocomposite Membrane of Poly(2,2-bis(trifluoromethyl)-4,5-difluoro-1,3-dioxole-co-tetrafluoroethylene) and Fumed Silica. *Macromolecules* **2005**, *38*, 3754−3764.
(8) Appel, M.; Fleischer, G.; Karger, J.; Dieng, A. C.; Riess, G. Investigation of the Restricted Diffusion in Spherical Cavities of Polymer by Pulsed Field Gradien Nuclear Magnetic Resonance. *Macromolecules* **1995**, *28*, 2345−2350.
(9) Kinning, D. J.; Thomasm, E. L.; Ottino, J. M. Effects of Morphology on the Transport of Gases in block Copolymers. *Macromolecules* **1987**, *20*, 1129−1133.
(10) Mortensen, K.; Brown, W. Poly(Ethylene Oxide)-Poly(Propylene Oxide)-Polyethylene Oxide) Triblock Copolymers in Aqueous Solution-the Influence of Relative Block Size. *Macromolecules* **1993**, *26*, 4128−4135.
(11) Fleischer, G.; Konak, C.; Puhlmann, A.; Rittig, F.; Karger, J. Dynamics of a Triblock Copolymer in a Selective Solvent for the Middle Block Investigated Using Pulsed field gradient NMR. *Macromolecules* **2000**, *33*, 7066−7071.
(12) Hamsley, I. W. *The Physics of Block Copolymer*; Oxford University Press: New York, 1998.
(13) Aggarwal, S. L. Structure and properties of block polymer and multiphase polymer systems. An overview of present status and future potential. *Polymer* **1976**, *17*, 938−56.
(14) Heck, B.; Arends, P.; Ganter, M.; Kressler, J.; Stuhn, B. SAXS and TEM Studies of Poly(styrene)-*block*-poly(ethene-*co*-but-1-ene)-*block*-poly(styrene) in Bulk and at Various Interfaces. *Macromolecules* **1997**, *30*, 4559−4566.
(15) Schneider, N. S.; Rivin, D. Solvent transport in hydrocarbon and perfluorocarbon ionomers. *Polymer* **2006**, *47*, 3119−3131.
(16) Kaur, S.; Florio, G.; Michalak, D. Cross-linking of sulfonated styreneethylene/butylene-styrene triblock polymer via sulfonamide linkages. *Polymer* **2002**, *43*, 5163−5167.
(17) As an example, 5 wt % toluene in PIB at 320 K is 1×10^{-7} cm^2 s^{-1}. Bandis, A.; Inglefield, P. T.; Jones, A. A.; Wen, W.-Y. A Nuclear Magnetic Resonance Study of Dynamics in Toluene-Polyisobutylene Solutions; 1. Pentrant Diffusion and Fujita Theory. *J. Polym. Sci., Polym. Phys.* **1995**, *33*, 1495−1503.
(18) As an example, hexane in PS is 10^{-13} cm^2 s^{-1}. Berens, A. R.; Hopfenberg, H. B. Diffusion of Organic Vapors at Low Concentration in Glassy PVC, Polystyrene and PMMA. *J. Membr. Sci.* **1982**, *10*, 283−303.
(19) Sax, J.; Ottino, J. M. Modeling of Transport of Samll Molecules in Polymer Blends:Applications of Effective Medium Theory. *Polym. Eng. Sci.* **1983**, *23*, 165−176.
(20) Giotto, M.; Lin, G.; Canfield, A.; Jones, A. A. Penetrant Diffusion in a Solid Ordered Triblock Copolymer. *Macromolecules* **2005**, *38*, 9904−9905.
(21) Mitra, P. P.; Sen, P. N.; Schwartz, L. M.; Le Doussal, P. Diffusion propagator as a probe of the structure of porous media. *Phys. Rev. Lett.* **1992**, *68*, 3555−3558.
(22) Latour, L. L.; Mitra, P. P.; Kleinberg, R. L.; Sotak, C. H. Time-dependent diffusion coefficient of fluids in porous media as a probe of surface-to-volume ratio. *J. Magn. Reson., Ser. A* **1993**, *101*, 342−346.
(23) Latour, L. L.; Kleinberg, R. L.; Mitra, P. P.; Sotak, C. H. Pore-size distributions and tortuosity in heterogeneous porous media. *J. Magn. Reson., Ser. A* **1995**, *112*, 83−91.
(24) Tanner, J. E.; Stejskal, E. O. Restricted Self-Diffusion of Protons in Colloidal Systems by the Pulsed-Gradient, Spin-Echo Method. *J. Chem. Phys.* **1968**, *49*, 1768−1777.
(25) Kuchel, P. W.; Lennon, A. J.; Durrant, C. J. Analytical Solutions and Simulations for Spin-Echo Measurements of Diffusion of Spins in a Sphere with Surface and Bulk Relaxation. *J. Magn. Reson.* **1996**, *B112*, 1−17.
(26) Soderman, O.; Jonsson, B. Restricted Diffusion in Cylindrical Geometry. *J. Magn. Reson.* **1995**, *A117*, 94−97.
(27) Lin, G.; Zhang, J.; Cao, H.; Jones, A. A. A Lattice Model for the Simulation of Diffusion In Heterogeneous Polymer Systems: Simulation of Apparent Diffusion constants As Determined by Pulse Field Gradient NMR. *J. Phys. Chem. B* **2003**, *107*, 6179−6186.
(28) Cicerone, M. T.; Wagner, P. A.; Ediger, M. D. Translational Diffusion on Heterogeneous Lattices: A Model for Dynamics in Glass Forming Materials. *J. Phys. Chem. B* **1997**, *101*, 8727.
(29) Price, W. S. Pulsed-Field Gradient Nuclear Magnetic Resonance as a Tool for Studying Translational Diffusion: Part 1. Basic Theory. *Concepts Magn. Reson.* **1997**, *9*, 299−336.
(30) Demco, D. E.; Rata, G.; Fechete, R.; Bluemich, B. Self-Diffusion Anisotropy of Small Penetrant Molecules in Deformed Elastomers. *Macromolecules* **2005**, *38*, 5647−5653.
(31) Helfand, E.; Wasserman, Z. R. Block Copolymer Theory. 6. Cylindrical Domains. *Macromolecules* **1980**, *13*, 994−998.
(32) Gido, S. P.; Gunther, J.; Thomas, E. L.; Hoffman, D. Lamellar Diblock Grain Boundary Morphology. 1. Twist Boundary Characterization. *Macromolecules* **1993**, *26*, 4506−4520.
(33) Rittig, F.; Fleischer, G.; Kärger, J.; Papadakis, C. M.; Almdal, K.; Štěpánek, P. Anistropic Self-Diffusion in a Hexagonally Ordered Asymmetric PEP-PDMS Diblock Copolymer Studied by Pulsed Field Gradient NMR. *Macromolecules* **1999**, *32*, 5872−5877.
(34) Min, B.; Qui, X. H.; Ediger, M. D.; Pitsikalis, M.; Hadjichristidis, N. *Macromolecules* **2001**, *34*, 4466−4475.
(35) Lutz, T. R.; He, Y.; Ediger, M. D.; Cao, H.; Lin, G.; Jones, A. A. *Macromolecules* **2003**, *36*, 1724−1730.

MA062619C